ANALYSIS OF STRAIN-RATE DEPENDENT MECHANICAL BEHAVIOR OF SINGLE CHONDROCYTE: A FINITE ELEMENT STUDY

TRUNG DUNG NGUYEN
School of Chemistry, Physics and Mechanical Engineering
Queensland University of Technology, Brisbane, Queensland, Australia
trungdung.nguyen@student.qut.edu.au

YUANTONG GU*
School of Chemistry, Physics and Mechanical Engineering
Queensland University of Technology, Brisbane, Queensland, Australia
Corresponding author: yuantong.gu@qut.edu.au

ADEKUNLE OLOYEDE
School of Chemistry, Physics and Mechanical Engineering
Queensland University of Technology, Brisbane, Queensland, Australia
k.oloyede@qut.edu.au

WIJITHA SENADEERA
School of Chemistry, Physics and Mechanical Engineering
Queensland University of Technology, Brisbane, Queensland, Australia
w3.senadeera@qut.edu.au

Various studies have been conducted to investigate the effects of impact loading on cartilage damage and chondrocyte death. These have shown that the rate and magnitude of the applied strain significantly influence chondrocyte death, and that cell death occurred mostly in the superficial zone of cartilage suggesting the need to further understand the fundamental mechanisms underlying the chondrocytes death induced at certain levels of strain-rate. To date there is no comprehensive study providing insight on this phenomenon. The aim of this study is to examine the strain-rate dependent behavior of a single chondrocyte using a computational approach based on Finite Element Method (FEM). An FEM model was developed using various mechanical models, which were Standard Neo-Hookean Solid (SnHS), porohyperelastic (PHE) and poroviscohyperelastic (PVHE) to simulate Atomic Force Microscopy (AFM) experiments of chondrocyte. The PVHE showed, it can capture both relaxation and loading rate dependent behaviors of chondrocytes, accurately compared to other models.

Keywords: Porohyperelastic, chondrocyte, Finite Element Method (FEM), biomechanics.

1. Introduction

Cartilage is the flexible connective tissue found in many parts of human and animal body such as nose, ear, elbow, knee and the joints between bones. Articular cartilage is the hyaline and avascular tissue that lines the surfaces of the diarthrodial joints. Its function is to provide a nearly frictionless bearing surface for the bones to transmit and distribute mechanical loads between them (Oloyede and Broom 1991, Oloyede and Broom 1996, Oloyede, Flachsmann and Broom 1992, Oloyede and Broom 1994a). Chondrocytes are cytoskeleton (CSK)-rich eukaryotic cells which are the mature cells in cartilage tissues and perform number of functions within the cartilage. The deterioration of the mechanical properties of these cells is believed to be one of the main factors in the development and progression of osteoarthritis (Jones et al. 1997, Trickey, Lee and Guilak

2000). Cellular behavior in response to external stimuli such as shear stress, fluid flow, osmotic pressure and mechanical loading have been investigated recently (Guilak, Erickson and Ting-Beall 2002, Ofek et al. 2010, Wu and Herzog 2006).

Physiological loads are usually applied at varying rates to achieve optimal biomechanical and biochemical outcomes in the body. Various studies have been conducted to investigate the effects of loading velocity on the mechanical responses of tissues and cells (Moo et al. 2012, Oloyede et al. 1992, Ewers et al. 2001, Kurz et al. 2001, Quinn et al. 2001, Radin, Paul and LowY 1970, Li et al. 2013). These researchers concluded that strain-rate and magnitude of loading greatly influence cell death (Kurz et al. 2001, Ewers et al. 2001). Typically, the response of cartilage can be transformed from the fluid-dominate to purely elastic behavior by changing the rate of loading (Oloyede et al. 1992, Oloyede and Broom 1993a). However, little research has been done to investigate the strain-rate dependent mechanical deformation properties of cartilage cells e.g. chondrocytes. It is believed that chondrocyte activity is regulated by its cellular mechanical environment (Shieh and Athanasiou 2003). The understanding of the strain-rate-dependent behavior of chondrocytes is arguably a significant contribution that would provide insight into chondrocyte health in particular and cartilage dysfunction in general.

There are several continuum mechanical models that have been developed for the single cell as well as other biological tissues. One of them is poroelastic field theory which is fundamental for Soil Mechanics (Biot 1941, Terzaghi 1943). But this has been modified and applied to cartilage which is a biological tissue (Higginson and Norman 1974, McCutchen 1998, Oloyede and Broom 1991, Oloyede and Broom 1996, McCutchen 1982). This poroelastic model considers soft tissues as porous materials consisting of a pore fluid that saturates the tissue and flows relative to the deformable porous elastic solid to describe their time-dependent response. This continuum model has been extended to account for the hyperelastic solid response which is non-linear material in the poroelastic formulation to give a porohyperelastic (PHE) material law (Simon and Gaballa 1989). Although the PHE model has been widely used and effective in tissue engineering i.e. articular cartilage (Oloyede and Broom 1991, Oloyede and Broom 1996), its application in the modeling of the single living cell has been significantly limited.

Because of recent advances in nanotechnology, a number of new experimental techniques for characterizing and studying the mechanical behavior of living cells have been developed. One such technique is Atomic Force Microscopy (AFM) which is a state-of-art experimental facility for high resolution imaging of tissues, cells and any surfaces as well as for probing mechanical properties of the samples both qualitatively and quantitatively (Touhami, Nysten and Dufrene 2003, Rico et al. 2005, Zhang and Zhang 2007, Lin, Dimitriadis and Horkay 2007, Kuznetsova et al. 2007, Faria et al. 2008). Its principle is to indent the cell with a tip of microscopic dimension which is attached to a very flexible cantilever and the force is measured from the deflection of the cantilever to obtain the force-indentation (F-δ) curve (Darling, Zauscher and Guilak 2006, Faria et al. 2008, Ladjal et al. 2009). This powerful tool is recently being used more and more widely for cell mechanics studies.

The aim of this study is to explore the strain-rate dependent mechanical behavior of a single chondrocyte using a computational approach based on FEM. A FEM model was developed using a number of mechanical models namely, Standard Neo-Hookean Solid

(SnHS), porohyperelastic (PHE) and poroviscohyperelastic (PVHE) to simulate the AFM evaluation of chondrocytes, where this was extended to the study of the changes in cell behavior with strain-rate.

2. Methodology

2.1. *Standard Neo-Hookean Solid (SnHS) model*

Viscoelastic model is one of the solid models which assume the cell to be a homogenous solid-like material. There are several models of viscoelasticity such as Maxwell, Voigt and the standard linear solid which consist of springs and dashpots (Fig. 1a-c). The springs are elastic (represented by the spring constant k) and the dashpots are viscous (represented by the viscosity μ), that is why they are called viscoelastic models.

In the differential form of linear viscoelasticity, the stress is expressed in terms of strain history with three material constants e.g. k_1, k_2 and μ as (Zhou, Lim and Quek 2005):

$$\mathbf{S} + \frac{\mu}{k_2}\dot{\mathbf{S}} = k_1\boldsymbol{\varepsilon} + \mu\left(1 + \frac{k_1}{k_2}\right)\dot{\boldsymbol{\varepsilon}} \tag{1}$$

$$\boldsymbol{\varepsilon} = \nabla\mathbf{u} + \nabla\mathbf{u}^T \qquad \dot{\boldsymbol{\varepsilon}} = \nabla\mathbf{v} + \nabla\mathbf{v}^T \qquad \mathbf{S} = \boldsymbol{\sigma} + p\mathbf{I} \tag{2}$$

where $\mathbf{S}$ is the deviatoric stress tensor, $\boldsymbol{\varepsilon}$ is the engineering strain tensor, which is the same as the deviatoric component under the condition of incompressibility, $\dot{\boldsymbol{\varepsilon}}$ is the engineering strain-rate tensor (the superposed dot denotes differentiation with respect to time), k_1 and k_2 are two elastic constants, μ is a viscous constant (see Fig. 1c)**,** $\mathbf{u}$ is the displacement field, $\mathbf{v}$ is the velocity field, $\boldsymbol{\sigma}$ is the total stress tensor, p is the hydrostatic pressure and $\mathbf{I}$ is the unit tensor.

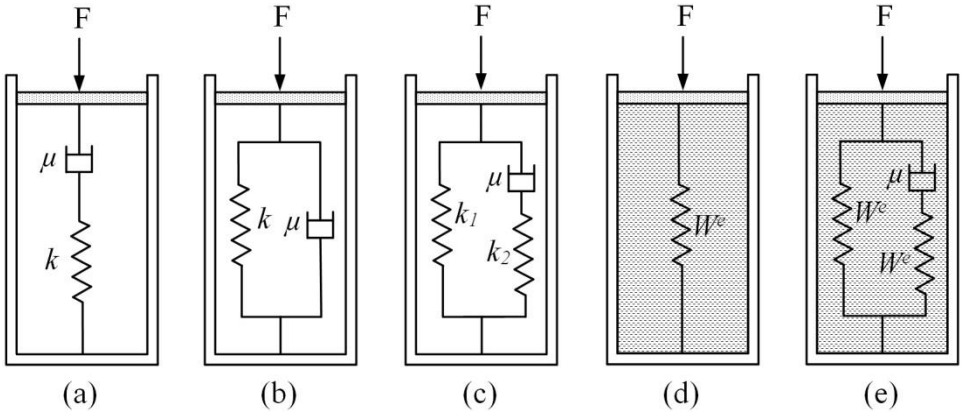

Figure 1. (a) Maxwell, (b) Voigt, (c) Standard linear solid (Fung 1965) viscoelastic models, (d) PHE model, and (e) PVHE model

In 2005, (Zhou et al. 2005) proposed a nonlinear viscoelastic model, namely the Standard Neo-Hookean Solid (SnHS) for the large deformation analysis of living cells, and is an extension of the Standard Linear Solid (SLS) viscoelasticity model. This model

replaced the linear elasticity elements in Fig. 1c by incompressible Neo-Hookean hyperelastic elements, leading to a simple constitutive law, where the strain energy density function of the incompressible material is:

$$U = \frac{G_0}{2}(I_1 - 3) \tag{3}$$

where G_0 is the shear modulus, I_1 is the deviatoric strain invariant, defined as:

$$I_1 = \lambda_1^2 + \lambda_2^2 + \lambda_3^2 \tag{4}$$

with λ_1, λ_2 and λ_3 being principal stretches. The deviatoric part **S** of the Cauchy stress tensor is:

$$\begin{aligned} \mathbf{S} &= G_0\left(\mathbf{B} - \frac{1}{3}I_1 \cdot \mathbf{I}\right) \\ \mathbf{B} &= \mathbf{F} \cdot \mathbf{F}^T \qquad \mathbf{F} = \frac{\partial \mathbf{x}}{\partial \mathbf{X}} \end{aligned} \tag{5}$$

where **S** is the deviatoric part of the Cauchy stress tensor, G_0 is the shear modulus, **F** is the deformation gradient of the current configuration **x** relative to the initial configuration **X**, and **B** is the left Cauchy-Green strain tensor.

This deviatoric part of the Cauchy stress tensor can further be written as:

$$\mathbf{S}(t) = \mathbf{S}_0(t) + \mathrm{SYM}\left[\int_0^t \frac{\dot{G}(s)}{G_0}\mathbf{F}_t^{-1}(t-s) \cdot \mathbf{S}_0(t-s) \cdot \mathbf{F}_t(t-s)ds\right] \tag{6}$$

$$\mathbf{F}_t(t-s) = \frac{\partial \mathbf{x}(t-s)}{\partial \mathbf{x}(t)}$$

where $\mathbf{F}_t(t-s)$ is the deformation gradient of the configuration $\mathbf{x}(t-s)$ at time $t-s$, relative to the configuration $\mathbf{x}(t)$ at time t , and $\mathbf{S}_0(t)$ represents the instantaneous stress caused by the deformation, which can be computed using Eq. (5), SYM[·] denotes the symmetric part of the matrix.

2.2. *Porohyperelastic (PHE) field theory*

In order to characterize and predict the finite strain and non-linear responses of structures, the porohyperelasticity (PHE) theory was developed as an extension of poroelastic theory (Simon and Gaballa 1989). This theory assumes that the chondrocyte is a continuum consisting of an incompressible hyperelastic porous solid skeleton saturated by an incompressible mobile fluid (Fig. 1d). Even though both solid and fluid are incompressible, the whole cell is compressible because of the volume loss of fluid during deformation. It has been applied in many engineering fields including Soil Mechanics (Sherwood 1993) and Biomechanics (Simon 1992, Meroi, Natali and Schrefler 1999, Nguyen 2005). The details of this theory are described clearly in the literature (Simon 1992, Simon et al. 1996, Simon et al. 1998b, Simon et al. 1998a, Kaufmann 1996). A summary of field equations for the isotropic form of this theory are stated below:

Conservation of linear momentum:

$$(\partial T_{ij})/(\partial X_j) = 0 \tag{7}$$

Conservation of fluid mass (Darcy's law):

$$\tilde{k}_{ij}\frac{\partial \pi^f}{\partial X_i} = \dot{\tilde{w}}_j \tag{8}$$

Conservation of (incompressible) solid and (incompressible) fluid mass is of the form:

$$\frac{\partial \dot{\tilde{w}}_i}{\partial X_k} + JH_{kl}\dot{E}_{kl} = 0 \tag{9}$$

where J, and $\dot{E}_{ij} = \frac{1}{2}(\frac{\partial x_k}{\partial X_i}\frac{\partial \dot{u}_k}{\partial X_j} + \frac{\partial x_k}{\partial X_j}\frac{\partial \dot{u}_k}{\partial X_i})$ are volume strain and rate of Green's strain.

Where the constitutive law:

$$\sigma_{ij} = \sigma^e_{ij} + \pi^f \delta_{ij}, \quad \sigma^e_{ij} = J^{-1}F_{im}S^e_{mn}F_{jn} \tag{10}$$

$$S_{ij} = S^e_{ij} + J\pi^f H_{ij}, \quad S^e_{ij} = \frac{\partial W^e}{\partial E_{ij}} \tag{11}$$

Where F_{ij}, T_{ij}, π^f, $\tilde{k}_{ij}$, $\dot{\tilde{w}}_j$, H_{ij}, S^e_{ij} and W^e are deformation gradient, first Piola-Kirchhoff total stress, fluid stress, symmetric permeability tensor, Lagrangian fluid velocity, Finger's strain, second Piola-Kirchhoff stress and effective strain energy density function, respectively. For simplicity, Neo-Hookean strain energy density function (Eq. 12) would be used in this study to represent the solid component of the cell (represented by the spring in Fig. 1d). The shadow part in Fig. 1d represents the fluid inside the cell.

2.3. *Poroviscohyperelastic (PVHE) field theory*

This PVHE model in this study is similar to the PHE model except that the solid component was modeled as Standard Neo-Hookean Solid (SnHS) viscoelasticity (Zhou et al. 2005). However, the SnHS model was modified by using the compressible Neo-Hookean model. The strain energy density function of this compressible material is:

$$W^e = C_1(\bar{I}_1 - 3) + \frac{1}{D_1}(J-1)^2 \tag{12}$$

where C_1 and D_1 are material constants, and J is the volume ratio.

As shown in Fig. 1e, the PVHE model consists of solid (SnHS model) and liquid (the shadow part in Fig. 1e) components. Note that the solid component of PVHE model is similar with the standard linear solid viscoelastic model in Fig. 1c. The difference is that the elastic spring element was replaced by the compressible Neo-Hookean model as mentioned above (Fig. 1e).

2.4. *Finite Element Method (FEM) model*

In this study, a Finite Element Method (FEM) model of a single chondrocyte to study its micro-deformation response by simulating atomic force microscopy (AFM) nano-indentation using the commercial software ABAQUS Standard version 6.9-1 (ABAQUS Inc., USA) (Fig. 2). Because both chondrocyte and AFM tip used are spherical, the axisymmetric element was used in this study to save computational cost (ABAQUS 1996). The model consists of a chondrocyte cell with a diameter of 14 µm which was indented to a maximum strain of 15% strain (corresponding to a displacement of approximately 2.1 µm). The specimen was indented with a colloidal probe of diameter 5 µm. In order to simulate correctly the AFM experiment, we created a loading element, namely, cantilever base (Fig. 2) and connected it to the colloidal probe with a spring element of spring constant 0.065 N/m. The simulation result was compared with that of AFM experiment in literature (Darling et al. 2006) to investigate the stress relaxation response of chondrocyte.

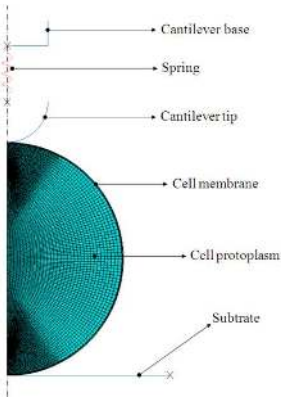

Figure 2. FEM model of single chondrocyte

Moreover, the chondrocyte was compressed at different loading rates to obtain insight into the effect of strain-rate on the biomechanical response of the cell. After compression, the displacement of the cantilever base was kept constant, while the chondrocyte was allowed to relax against it over time. Fig. 3 presents a typical displacement plot of the cantilever base. The model considered the cell as SnHS, PHE and poroviscohyperelastic (PVHE) and the results were cross compared against one another. The main difference in these FEM models was that the cell membrane was not considered in SnHS model, but included in the other two models since the hydraulic permeability of cell protoplasm and membrane are different (Ateshian, Costa and Hung 2007, Moo et al. 2012).

After the analysis, the displacements of the cantilever base and the probe were extracted and used to calculate the deflection of the cantilever. The deflection is multiplied by the spring constant to obtain force applied to the cell as follows:

$$F = k_c(d_{base} - d_{bead}) \tag{13}$$

where k_c is the spring constant of the cantilever (e.g. 0.065 N/m in this study), d_{base} and d_{bead} are displacements of the cantilever base and tip, respectively.

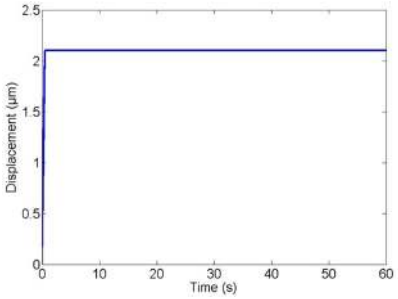

Cantilever base displacement

Time (sec)	Displacement (μm)
0	0
0.5 (*)	2.1
60	2.1

(*) will be changed to account for the effect of strain rate

Figure 3. Plot of cantilever base movement

2.4.1. *Standard Neo-Hookean Solid (SnHS) model*

Firstly, the FEM model of chondrocyte is created to simulate AFM experiment and the results are compared to those published in the literature (Darling et al. 2006) to validate the model. This FEM model is different from that in Fig. 2 because it does not contain a component representing cell membrane. Four-node quadrilateral axisymmetric stress element was used in this study (totally 7342 elements were used). The chondrocyte is simulated with a SnHS material model and is indented to 15% of the cell diameter in 0.5 s (see Fig. 3) using ABAQUS. The material parameters are presented in Table 1 and are extracted from an earlier paper (Darling et al. 2006).

Table 1. SnHS, PHE and PVHE material properties adopted in this study

	SnHS	PHE		PVHE	
		Protoplasm	Membrane	Protoplasm	Membrane
Young's modulus (Pa)	650	610	10,000	610	10,000
Poisson ratio	0.38	0.38	0.38	0.38	0.38
Prony coefficient g_1	0.4138	N/A	N/A	0.31	0.31
Prony coefficient λ_1 (s)	5.2	N/A	N/A	1.5	1.5
Permeability (m^4/N.s)	N/A	0.6×10^{-15}	3×10^{-21}	0.6×10^{-15}	3×10^{-21}
Void ratio	N/A	4	3	4	3

2.4.2. *PHE model*

Our PHE model consists of cell protoplasm, cell membrane, cantilever tip, cantilever base, and plate (see Fig. 2). Eight-node quadrilateral axisymmetric pore fluid/stress element was used in this study (totally 9470 and 222 elements were used for chondrocyte and its membrane, respectively). The protoplasm and membrane's material properties are shown in Table 1, and the rest of the components were assumed to be rigid bodies. The Young's modulus and Poisson's ratio are assumed to be the same for both protoplasm and membrane. Also, the hydraulic permeability of the membrane is assumed to be 6 orders smaller than that of the protoplasm (Ateshian et al. 2007, Moo et al. 2012). The transient poroelastic analysis was used to study the deformation mechanics of the chondrocyte cell.

2.4.3. *PVHE model*

The adopted PVHE model is similar to the PHE model where the solid component was modeled as a Standard Neo-Hookean Solid (SnHS) viscoelasticity material (Zhou et al.

2005). Eight-node quadrilateral axisymmetric pore fluid/stress element was used in this study (totally 9470 and 222 elements were used for chondrocyte and its membrane, respectively). The protoplasm and membrane's material properties are provided in table 1. All other components are assumed to be rigid bodies. The inverse finite element approach was used to estimate cell viscoelastic properties of the cell under this model (Zhao, Wyss and Simmons 2009).

3. Results and Discussion

3.1. *Standard Neo-Hookean Solid (SnHS) model*

The von Mises stress distribution obtained in the SnHS analyses is shown in Fig. 4. The results presented represent the unloaded behaviors, deformation and relaxation responses of the various models (Fig. 4) (the measurement unit was MPa). As would be expected the results in Fig. 4, demonstrate that during indentation the stress increased and was concentrated near the colloidal probe and substrate and then reduced during relaxation.

The force-time and force-indentation (F-δ) curves are presented in Fig. 5. Fig. 5a and 5c were extracted from FEM model and Fig. 5b and 5d were obtained from published data (Darling et al. 2006) from their AFM experiments. As can be observed from Fig. 5a and b, the simulation results significantly agree with the AFM experimental results. These results validate our model demonstrating its capacity to accurately simulate existing experimental results. It is interesting to note that the FEM result in Fig. 5c was different from the experimental data published in (Darling et al. 2006). The reason is explained as follow.

Darling et al. presented that most of cell was indented to 1.3-2.1 μm in their experiments corresponding to around 15% of the cell height of around 12-15 μm. The cell height in this study was 14 μm which is the average value, thus 15% of the cell height would be 2.1 μm. Hence, the result presented in Fig. 5d where the cell was indented to around 2.4 μm might be of a large cell (cell height was around 16 μm) with the elastic modulus was determined to be 380 Pa which is much smaller than average modulus of 610 ± 340 Pa (Darling et al. 2006). In this study, we thus increased the modulus to 650 Pa so that the maximum force was around 3.5 nN with the indentation of 2.1 μm to be comparable with the relaxation results presented in Fig. 5b (Darling et al. 2006). Note that our modulus was very close to their published result, so we believe that our model can represent the average behavior of chondrocytes. The results of this model will be used as reference for other two models.

In order to investigate the cell response with respect to strain-rate, the cell was indented to 15% of its diameter at varying durations of between 0.03 and 3s, followed by a 60s stress relaxation phase. Thus, the strain-rate was varied from 5 %/s to 500 %/s of the cell diameter. The results for different rates are summarized in Fig. 6 for deformation over a period of 6s for a clear illustration. All the curves converged to the same equilibrium force of 2.28 nN. Moreover, the maximum value of the reaction force was practically constant with the strain-rates investigated, and after indentation the force decreases indicating the relaxation phase; the reason for this relaxation behavior is because the cell becomes softer with time. Although the SnHS model can capture the maximum and asymptotic value of force, the relaxation time is longer than that observed in the

experiment. This could be argued to be a consequence of the gradual reduction in the shear relaxation modulus with time (Zhou et al. 2005). Moreover, this model assumes that the cell is solid, whereas, a cell should be more appropriately represented as a system consisting of a solid skeleton and mobile fluid. In order to address this limitation, an improved FEM model with PHE material and the same material properties as those of SnHS model was developed as discussed below.

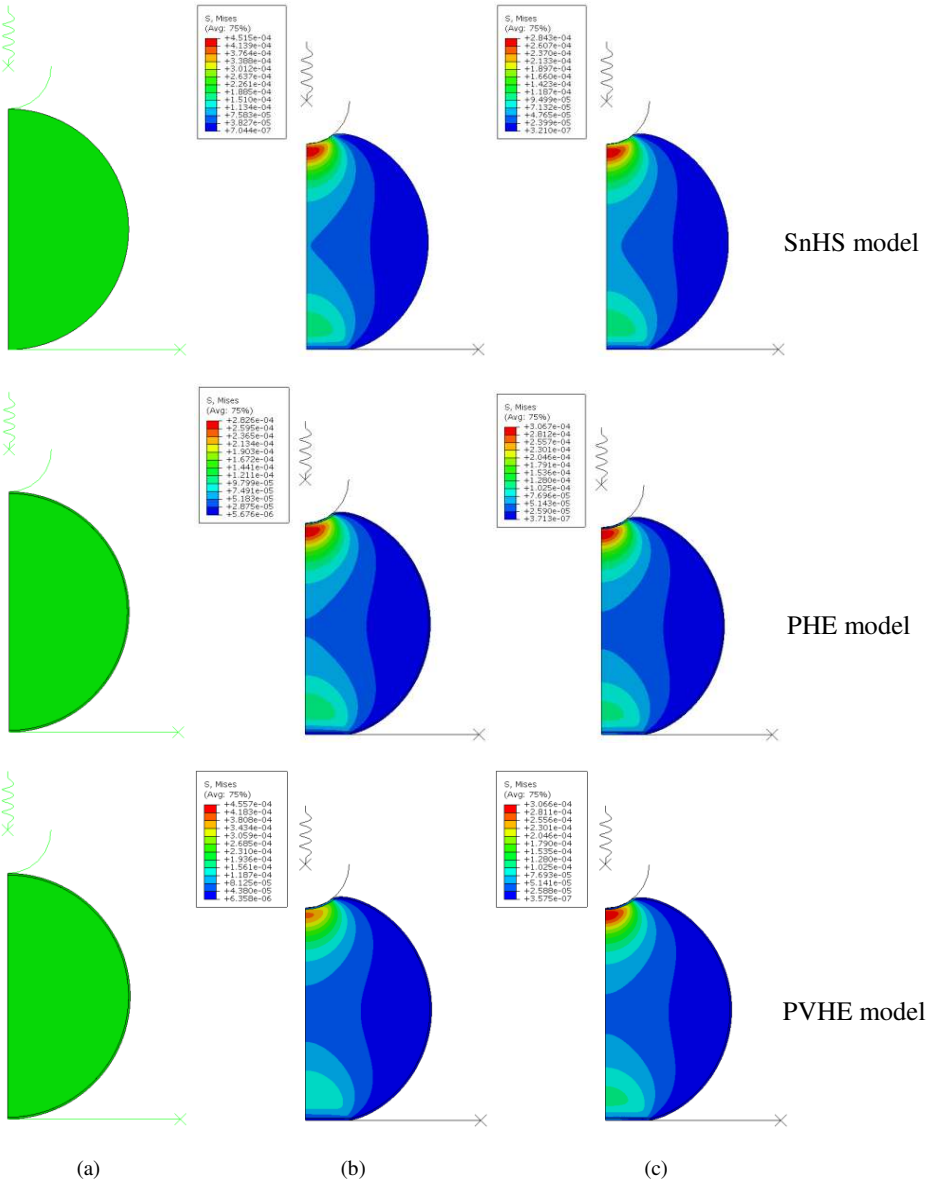

Figure 4. von Mises stress distribution of FEM chondrocyte's deformation using SnHS, PHE and PVHE material models under 30 %/s strain-rate (a) in the unloaded condition, (b) indented state and (c) during relaxation

3.2. *PHE model*

Fig. 7 shows the force-time and force-indentation (F-δ) curves extracted from PHE FEM model for a strain–rate of 30 %/s of the cell diameter. As seen in Fig. 7a, the applied force reached a maximum value and then decreased to its equilibrium value. This is the effect of fluid loss from the cell especially in the relaxation phase. The reason is that hydraulic permeability of cell membrane is much lower than that of cell protoplasm e.g. around 5 orders smaller. This caused the fluid difficult to transport through the membrane. However, the maximum value of the force applied is different with that of experimental result shown in Fig. 5b. Thus, we hypothesized that the behaviors of chondrocytes are influenced by not only the interaction between solid and fluid components but also the intrinsic viscoelasticity of solid component (Baaijens et al. 2005, Trickey et al. 2006, Shieh, Koay and Athanasiou 2006, Mow et al. 1980).

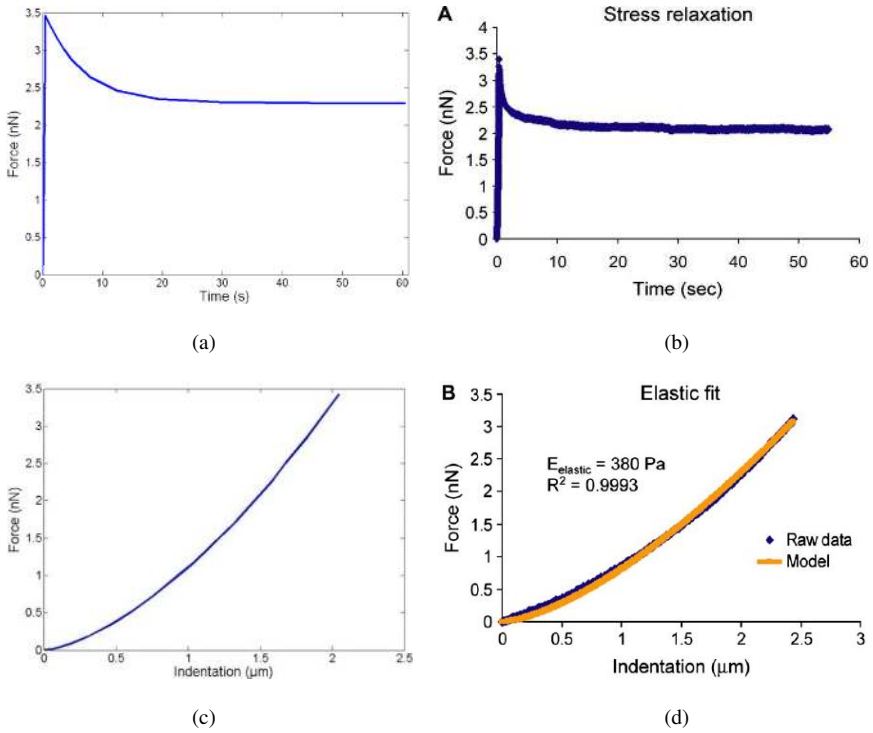

Figure 5. (a), (c) Force-time and force-indentation (F-δ) curves extracted from SnHS FEM model; (b), (d) Force-time and force-indentation (F-δ) curves obtained from AFM experiment in case of 30 %/s strain-rate (Darling et al. 2006)

The von Mises or solid skeleton stress and pore pressure distributions are shown in Figs. 4 and 8, respectively. Fig. 9 shows pore pressure-time variation measured at a node in inner membrane. As can be observed from Fig. 8 and 9, the fluid pore pressure increased to its maximum value at maximum strain before decay to it minimum value while the solid skeleton stress increased (see Fig. 4). This is the fluid exudation stage of the deformation. Those results are similar to cartilage responses as published in (Oloyede and Broom 1993b, Oloyede and Broom 1994b, Oloyede and Broom 1996, Oloyede et al.

1992). This is the stress-sharing mechanism in porous medium where the applied stress is firstly taken by the fluid and then transferred from fluid to solid in the later stage.

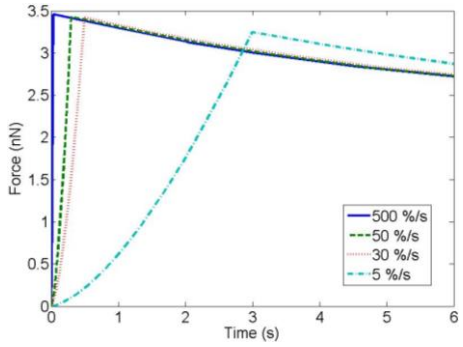

Figure 6. AFM force-time curves extracted from FEM SnHS model of chondrocyte with strain-rate from 5 s^{-1} to 0.05 s^{-1}. The maximum time is limited to 6 seconds for clearer illustration

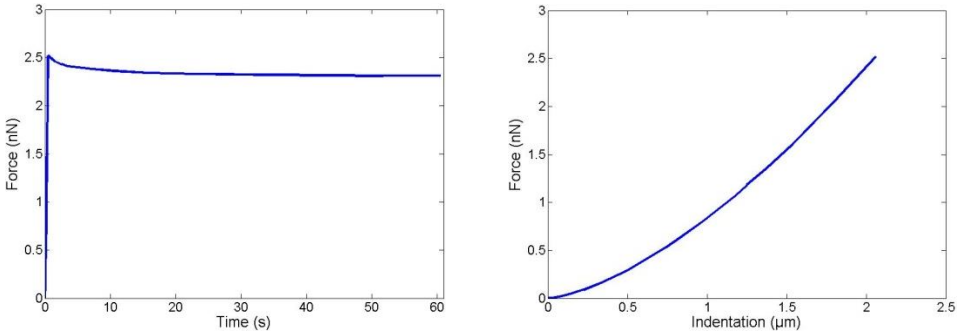

(a) (b)

Figure 7. (a) Force-time and (b) force-indentation (F-δ) curves extracted from PHE FEM model in case of 30 %/s strain-rate

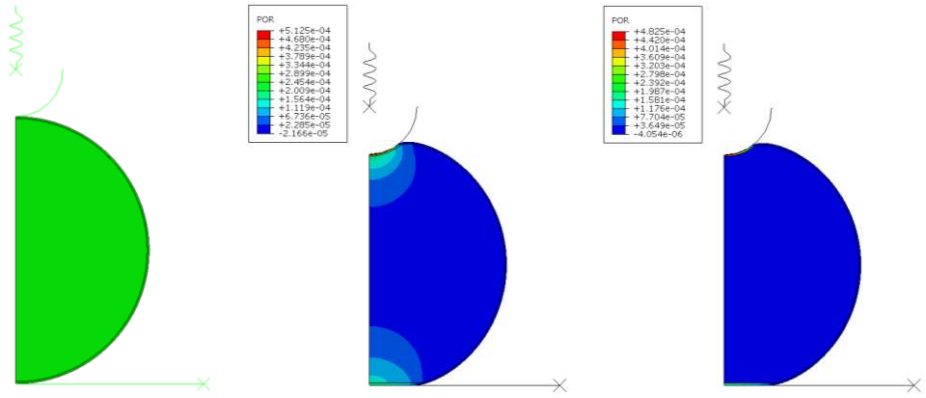

(a) (b) (c)

Figure 8. Pore pressure distribution of FEM chondrocyte model using PHE material in case of 30 %/s strain-rate (a) before indentation, (b) after indentation and (c) after relaxation

In order to elucidate the strain-rate dependent biomechanics of the cell, we indented the single chondrocyte at different strain-rate from 5 %/s to 500 %/s of the cell diameter as the same with SnHS material model (see Fig 10). The response demonstrates that the maximum values of force decreased slightly with reduction in strain-rate, while the maximum force reduces to an asymptotical value similarly to the behavior of the SnHS model. This response occurred when the pore pressure inside the cell decays to zero. We can observe that the maximum values of force applied on the chondrocyte are larger with higher strain-rate. This is because of the effect of water being trapped within the cell due to its inability to escape from the matrix quick enough at the high levels of strain-rate of up to 500%/s applied. After that when the displacement of cantilever tip is kept constant, the pressure difference between inside and outside of the cell drives the fluid to flow and this causes the fluid exudation stage of the deformation.

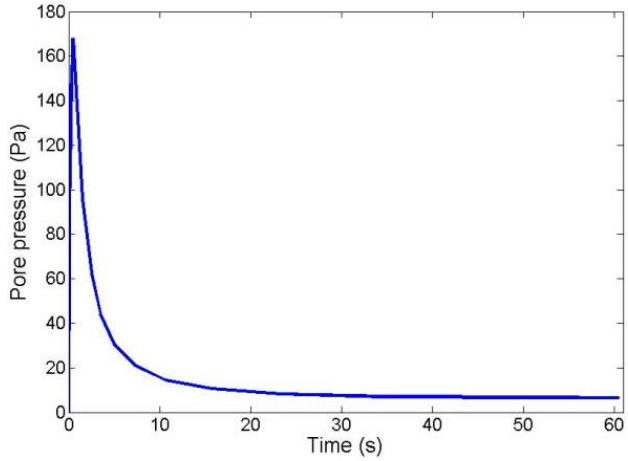

Figure 9. Pore pressure vs time curve of PHE model in case of 30 %/s strain-rate

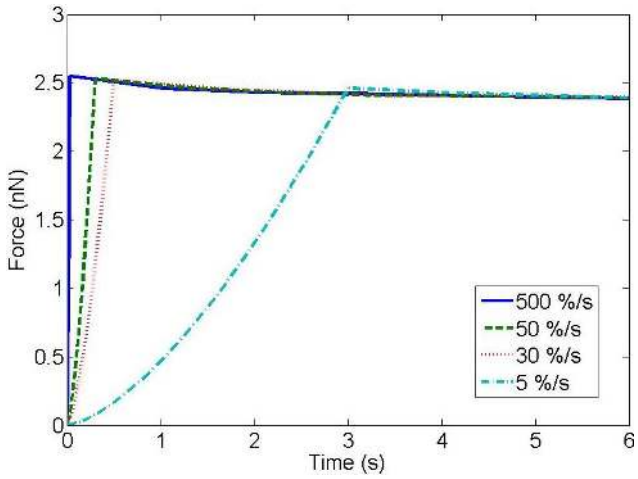

Figure 10. AFM force-time curves extracted from FEM PHE model of chondrocyte with strain-rate from 5 s^{-1} to 0.05 s^{-1}. The maximum time is limited to 6 seconds for clearer illustration

3.3. *PVHE model*

As mentioned above, the mechanical responses of chondrocytes are likely dependent on both fluid-solid interaction and intrinsic viscoelasticity of solid. Thus, PVHE model was developed in this study. The force-time and force-indentation curves are shown in Fig. 11 which have a good agreement with experiments (see Fig. 5). It is interesting to note that although SnHS model could simulate stress relaxation response of chondrocyte, the relaxation time was likely larger than experiment. On the other hand, the PVHE model had a smaller relaxation time which is close to experimental result. This is because the pore fluid responded rapidly and exuded through the membrane right after indentation phase.

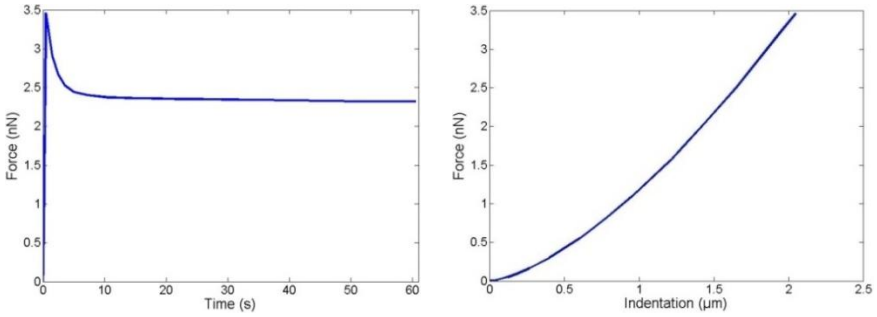

(a) (b)

Figure 11. (a) Force-time and (b) force-indentation (F-δ) curves extracted from PVHE FEM model in case of 30 %/s strain-rate

As we can see from Fig. 4, the von Mises or solid skeleton stress concentration shows both stress relaxation and stress sharing mechanisms. Fig. 12 and 13 plot pore pressure distribution and pore pressure-time curve, respectively which are similar to those of PHE model. The difference is that maximum pore pressure of PVHE model is higher than that of PHE model. This is because the viscohyperelastic material has a larger shear modulus compared to the hyperelastic one in the transient response (see Fig. 7 and 11).

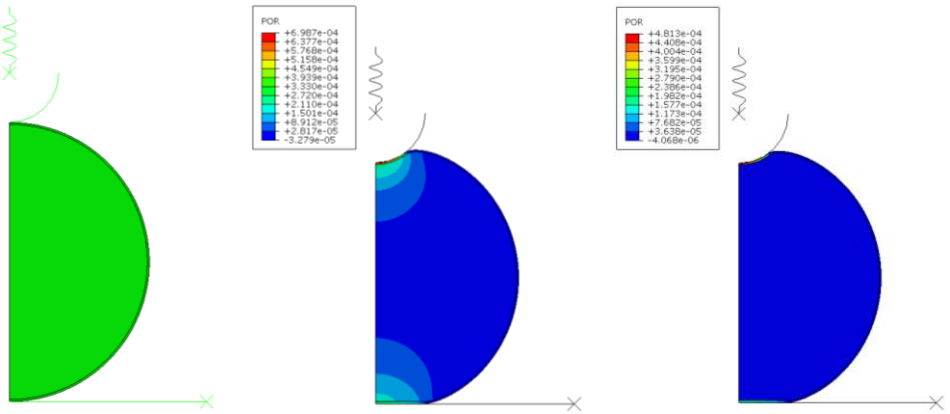

(a) (b) (c)

Figure 12. Pore pressure distribution of FEM chondrocyte model using PVHE material in case of 30 %/s strain-rate (a) before indentation, (b) after indentation and (c) after relaxation

Fig. 14 shows the force-time curves with different strain-rate from 5 %/s to 500 %/s. We can observe that the maximum force applied reduced significantly with decreasing of strain-rate. This effect which is dominated to strain-rate behavior of chondrocyte is the same with that of PHE model but more predominant. Thus, this PVHE model can capture the loading rate dependent behavior better than PHE model and the relaxation behavior better than SnHS model. Hence, the PVHE model is recommended. Note that the calculate time for PVHE is similar to that of SnHS and PHE models.

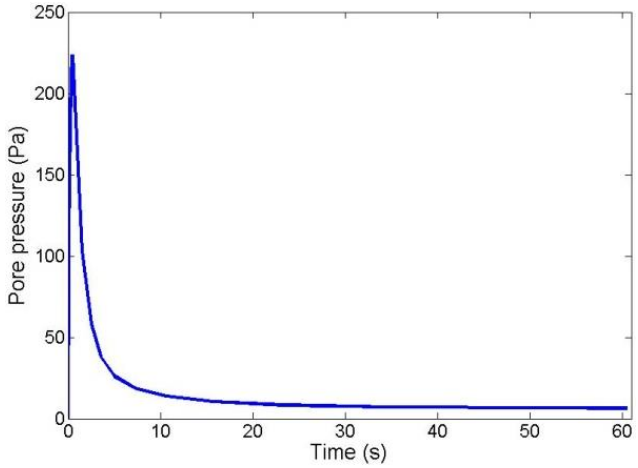

Figure 13. Pore pressure vs time curve of PVHE model in case of 30 %/s strain-rate

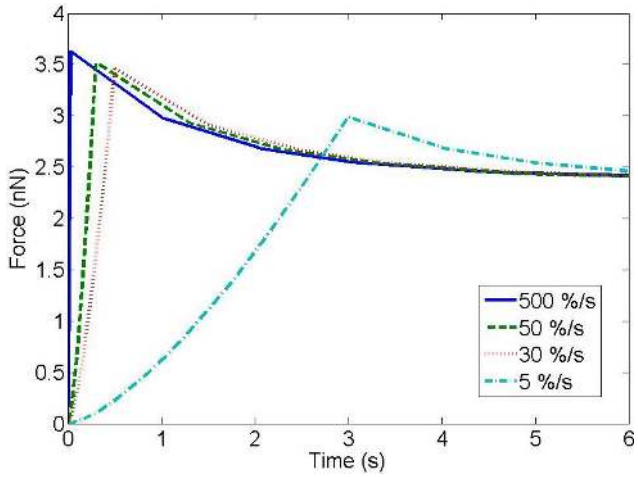

Figure 14. AFM force-time curves extracted from FEM PVHE model of chondrocyte with strain-rate from 5 s^{-1} to 0.05 s^{-1}. The maximum time is limited to 6 seconds for clearer illustration

4. Conclusions

This study has developed an FEM model to simulate AFM experiment of single chondrocyte using three material models e.g. Standard Neo-Hookean Solid (SnHS), porohyperelastic (PHE) and poroviscohyperelastic (PVHE). The chondrocyte was

subjected to various strain-rates from 5 %/s to 500 %/s to study its strain-rate dependent mechanical behavior. There are several conclusions drawn from the study and given below:

- SnHS model: this model is able to capture maximum and equilibrium force applied values as well as strain-rate dependent mechanical response of chondrocyte. Moreover, the relaxation behavior is because of viscoelasticity. However, the relaxation time is likely longer than experimental result.
- PHE model: although this model could not capture the maximum applied force, the equilibrium one agrees well with experimental result. In addition, the relaxation phenomenon due to the effect of volume loss of fluid could be simulated in this model based on fluid pore pressure distribution and pore pressure-time curve. Thus, the relaxation behavior is because of stress sharing mechanism between solid and fluid components.
- PVHE model: this model has advantages of both previous models. The relaxation behavior in this model is because of both viscoelasticity of solid component and stress sharing mechanism between solid and fluid constituents. The maximum and equilibrium applied force values as well as relaxation time of this model agree with experimental results very well. It can also capture the loading rate dependent mechanical behavior of chondrocyte. Therefore, this model is recommended.

PHE/PVHE models have been applied in a variety of biomechanical studies yielding reasonable and acceptable results. With this approach, we can have a clear insight into the consolidation as well as swelling behaviors of the cell. Despite of many advances, to our knowledge, these PHE/PVHE models have not been used widely for studying living cell mechanics particularly chondrocyte, especially PVHE model. Thus, this study would be the first one to use this PVHE model for chondrocytes with FEM as a simulation tool. The PVHE has been proven to be the most suitable model for single chondrocyte. This will open a big avenue for us to explore the biomechanical properties of chondrocytes. In future, other biochemical behaviors of chondrocyte such as swelling behavior will be accounted for in the PVHE model. Also, AFM experiments with different loading rates will be conducted to validate the PVHE model.

Acknowledgement

This research was funded by ARC Future Fellowship project and QUT Postgraduate Research Scholarship. The authors would like to thank Dr. Sanjleena Singh for advices in experimental techniques.

References

ABAQUS. 1996. *ABAQUS/Standard User's Manual (version 5.6)*. Hibbitt, Karlsson, and Sorensen, Inc., Pawtucket, USA.

Ateshian, G. A., K. D. Costa & C. T. Hung (2007) A theoretical analysis of water transport through chondrocytes. *Biomech Model Mechanobiol,* 6**,** 91-101.

Baaijens, F. P. T., W. R. Trickey, T. A. Laursen & F. Guilak (2005) Large Deformation Finite Element Analysis of Micropipette Aspiration to Determine the Mechanical Properties of the Chondrocyte. *Annals of Biomedical Engineering,* 33**,** 494-501.

Biot, M. A. (1941) General Theory of Three-Dimensional Consolidation. *Journal of Applied Physics,* 12**,** 155-164.

Darling, E. M., S. Zauscher & F. Guilak (2006) Viscoelastic properties of zonal articular chondrocytes measured by atomic force microscopy. *Osteoarthritis and Cartilage,* 14**,** 571-579.

Ewers, B. J., D. Dvoracek-Driksna, M. W. Orth & R. C. Haut (2001) The extent of matrix damage and chondrocyte death in mechanically traumatized articular cartilage explants depends on rate of loading. *Journal of Orthopaedic Research,* 19**,** 779-784.

Faria, E. C., N. Ma, E. Gazi, P. Gardner, M. Brown, N. W. Clarke & R. D. Snook (2008) Measurement of elastic properties of prostate cancer cells using AFM. *Analyst,* 133**,** 1498-1500.

Fung, Y. C. 1965. Foundations of Solid Mechanics. Englewood Cliffs, New Jersey: Prentice-Hall, Inc.

Guilak, F., G. R. Erickson & H. P. Ting-Beall (2002) The Effects of Osmotic Stress on the Viscoelastic and Physical Properties of Articular Chondrocytes. *Biophysical Journal,* 82**,** 720-727.

Higginson, G. R. & R. Norman (1974) The Lubrication of Porous Elastic Solids with Reference to the Functioning of Human Joints. *Journal of Mechanical Engineering Science,* 16**,** 250-257.

Jones, W. R., H. P. Ting-Beall, G. M. Lee, S. S. Kelley, R. M. Hochmuth & F. Guilak. 1997. Mechanical Properties of Human Chondrocytes and Chondrons from Normal and Osteoarthritic Cartilage. In *43rd Annual Meeting, Orthopaedic Research Society*. San Francisco, California.

Kaufmann, M. V. 1996. Porohyperelastic Analysis of Large Arteries Including Species Transport and Swelling Effects. In *Mechanical Engineering*. The University of Arizona, Tucson, AZ.

Kurz, B., M. Jin, P. Patwari, D. M. Cheng, M. W. Lark & A. J. Grodzinsky (2001) Biosynthetic response and mechanical properties of articular cartilage after injurious compression. *Journal of Orthopaedic Research,* 19**,** 1140-1146.

Kuznetsova, T. G., M. N. Starodubtseva, N. I. Yegorenkov, S. A. Chizhik & R. I. Zhanov (2007) Atomic force microscopy probing of cell elasticity

Micron, 38**,** 824-833.

Ladjal, H., J. L. Hanus, A. Pillarisetti, C. Keefer, A. Ferreira & J. P. Desai. 2009. Atomic Force Microscopy-Based Single-Cell Indentation: Experimentation and Finite Element Simulation. In *IEEE/RSJ International Conference on Intelligent Robots and Systems*. St. Louis, MO: Univted States.

Li, T., Y. T. Gu, X. Q. Feng, P. K. D. V. Yarlagadda & A. Oloyede (2013) Hierarchical multiscale model for biomechanics analysis of microfilament networks. *Journal of Applied Physics,* 113**,** 194701-194701-7.

Lin, D. C., E. K. Dimitriadis & F. Horkay (2007) Elasticity of rubber-like materials measured by AFM nanoindentation. *eXPRESS Polymer Letters,* 1**,** 576-584.

McCutchen, C. W. (1982) Cartilage is poroelastic, not viscoelastic (including and exact theorem about strain energy and viscous loss, and an order of magnitude relation for equilibration time). *Journal of Biomechanics,* 15**,** 325–327.

--- (1998) Consolidation theory derived without invoking porosity. *International Journal of Solids and Structures,* 35**,** 69–81.

Meroi, E. A., A. N. Natali & B. A. Schrefler (1999) A Porous Media Approach to Finite Deformation Behaviour in Soft Tissues. *Computer Methods in Biomechanics and Biomedical Engineering,* 2**,** 157-170.

Moo, E. K., W. Herzog, S. K. Han, N. A. Abu Osman, B. Pingguan-Murphy & S. Federico (2012) Mechanical behaviour of in-situ

chondrocytes subjected to different loading rates: a finite element study. *Biomech Model Mechanobiol,* 11**,** 983-993.

Mow, V. C., S. C. Kuei, W. M. Lai & C. G. Armstrong (1980) Biphasic creep and stress relaxation of articular cartilage in compression_Theory and experiments. *Journal of Biomechanical Engineering,* 102**,** 73-84.

Nguyen, T. C. 2005. Mathematical Modelling of the Biomechanical Properties of Articular Cartilage. In *School of Mechanical, Manufacturing and Medical Engineering*. Brisbane, Australia: Queensland University of Technology.

Ofek, G., E. Dowling, R. Raphael, J. McGarry & K. Athanasiou (2010) Biomechanics of single chondrocytes under direct shear. *Biomechanics and Modeling in Mechanobiology,* 9**,** 153-162.

Oloyede, A. & N. Broom (1993a) Stress-sharing between the fluid and solid components of articular cartilage under varying rates of compression. *Connective tissue research,* 30**,** 127.

Oloyede, A. & N. D. Broom (1991) Is classical consolidation theory applicable to articular cartilage deformation? *Clinical Biomechanics,* 6**,** 206–212.

--- (1993b) A Physical Model for the Time-Dependent Deformation of Articular Cartilage. *Connective Tissue Research,* 29**,** 251-261.

--- (1994a) Complex nature of stress inside loaded articular cartilage. *Clinical Biomechanics,* 9**,** 149-156.

--- (1994b) The Generalized Consolidation of Articular Cartilage: An Investigation of Its Near-Physiological Response to Static Load. *Connective Tissue Research,* 31**,** 75-86.

--- (1996) The Biomechanics of Cartilage Load-Carriage. *Connective Tissue Research,* 34**,** 119-143.

Oloyede, A., R. Flachsmann & N. D. Broom (1992) The Dramatic Influence of Loading Velocity on the Compressive Response of Articular Cartilage. *Connective Tissue Research,* 27**,** 211-224.

Quinn, T. M., R. G. Allen, B. J. Schalet, P. Perumbuli & E. B. Hunziker (2001) Matrix and cell injury due to sub-impact loading of adult bovine articular cartilage explants: effects of strain rate and peak stress. *Journal of Orthopaedic Research,* 19**,** 242-249.

Radin, E. L., I. L. Paul & M. LowY (1970) A comparison of the dynamic force transmitting properties of subchondral bone and articular cartilage. *The Journal of Bone & Joint Surgery,* 52**,** 444-456.

Rico, F., P. Roca-Cusachs, N. Gavara, R. Farre, M. Rotger & D. Navajas (2005) Probing mechanical properties of living cells by atomic force microscopy with blunted pyramidal cantilever tips. *Physical Review,* 72**,** 1-10.

Sherwood, J. D. (1993) Biot poroelasticity of a chemically active shale. *Proc. R. Soc. Lond. A,* 440**,** 365-377.

Shieh, A. C. & K. A. Athanasiou (2003) Principles of cell mechanics for cartilage tissue engineering. *Annals of biomedical engineering,* 31**,** 1-11.

Shieh, A. C., E. J. Koay & K. A. Athanasiou (2006) Strain-dependent recovery behavior of single chondrocytes. *Biomechan Model Mechanobiol,* 5**,** 172-179.

Simon, B. R. (1992) Multiphase Poroelastic Finite Element Models for Soft Tissue Structures. *Applied Mech. Rev.,* 45**,** 191-219.

Simon, B. R. & M. A. Gaballa (1989) Total Lagrangian 'porohyperelastic' finite element models of soft tissue undergoing finite strain.pdf. *1989 advances in bioengineering, B Rubinsky (ed),* BED-vol 15, ASME, New York**,** 97-98.

Simon, B. R., M. V. Kaufmann, M. A. McAfee & A. L. Baldwin (1998a) Porohyperelastic finite element analysis of large arteries using ABAQUS. *ASME Journal of Biomechanical Engineering,* 120**,** 296-298.

Simon, B. R., M. V. Kaufmann, M. A. McAfee, A. L. Baldwin & L. M. Wilson (1998b) Identification and Determination of Material Properties for Porohyperelastic Analysis of Large Arteries. *ASME Journal of Biomechanical Engineering,* 120**,** 188-194.

Simon, B. R., J. P. Liable, D. Pflaster, Y. Yuan & M. H. Krag (1996) A Poroelastic Finite Element Formulation Including Transport and Swelling in Soft Tissue Structures. *Journal of Biomechanical Engineering,* 118**,** 1-9.

Terzaghi, K. 1943. *Theoritical Soil Mechanics*. John Wiley, New York.

Touhami, A., B. Nysten & Y. F. Dufrene (2003) Nanoscale mapping of the elasticity of microbial cells by atomic force microscopy. *Langmuir,* 19**,** 4539-4543.

Trickey, W. R., F. P. T. Baaijens, T. A. Laursen, L. G. Alexopoulos & F. Guilak (2006) Determination of the Poisson's ratio of the cell: recovery properties of chondrocytes after release from complete micropipette aspiration. *Journal of Biomechanics,* 39**,** 78-87.

Trickey, W. R., G. M. Lee & F. Guilak (2000) Viscoelastic Properties of Chondrocytes from Normal and Osteoarthritic Human Cartilage. *Journal of Orthopaedic Research,* 18**,** 891-898.

Wu, J. Z. & W. Herzog (2006) Analysis of the mechanical behavior of chondrocytes in unconfined compression tests for cyclic loading. *Journal of Biomechanics,* 39**,** 603-616.

Zhang, C. Y. & Y. W. Zhang (2007) Effects of membrane pre-stress and intrinsic viscoelasticity on nanoindentation of cells using AFM. *Philosophical Magazine,* 87**,** 3415-3435.

Zhao, R., K. Wyss & C. A. Simmons (2009) Comparison of analytical and inverse finite element approaches to estimate cell viscoelastic properties by micropipette aspiration. *Journal of Biomechanics,* 42**,** 2768–2773.

Zhou, E. H., C. T. Lim & S. T. Quek (2005) Finite Element Simulation of the Micropipette Aspiration of a Living Cell Undergoing Large Viscoelastic Deformation. *Mechanics of Advanced Materials and Structures,* 12**,** 501-512.